

# Binary Janus Porous Coordination Polymer Coatings for Sensor Devices with Tunable Analyte Affinity\*\*

Mikhail Meilikhov, Shuhei Furukawa,\* Kenji Hirai, Roland A. Fischer, and Susumu Kitagawa\*

Heterogeneous functional materials, in which multiple molecular architectures are combined at nano/meso/macro scales, have attracted significant attention because of the collective and nonlinear functionality of the entire systems, which are controlled by the active interactions of single components.<sup>[1]</sup> The overall performance strongly depends on spatial configuration of single components as it was shown for block copolymers.<sup>[2]</sup> Regarding binary systems of heterogeneous materials, two different symmetric arrangements are known: centrosymmetric and non-centrosymmetric materials (Figure 1). Besides the fact that a centrosymmetric core-shell configuration gives promising collective properties, as shown for different types of materials such as metal particles,

metal oxides, or block copolymers,<sup>[3]</sup> the absence of centrosymmetry can induce higher diversity and complexity in the system as seen in biological systems.<sup>[4]</sup> However, the synthesis of non-centrosymmetric systems such as Janus materials is still challenging because of the complexity to control the assembly of building units in an anisotropic way.<sup>[5]</sup>

The introduction of permanent porosity into a heterogeneous material would result in additional properties owing to its molecular interaction with guest species.<sup>[6]</sup> For instance, the integration of compartments with different permeability characteristics into one heterogeneous porous material would enhance the overall performance in applications such as separation and selective adsorption.<sup>[7]</sup> Porous coordination polymers (PCPs), assembled from organic linkers and metal ions, have shown high potential for a variety of applications in gas storage and separation, catalysis, sensing, and delivery of bioactive molecules.<sup>[8]</sup> Since by simple replacement of molecular building units the porous property can be tuned without alteration of the overall framework structure, PCPs are suitable for the fabrication of heterogeneous porous materials. Indeed, heterostructured PCP materials containing two distinct framework structures were synthesized by using the hetero-epitaxial growth method.<sup>[9]</sup> We recently demonstrated that the formation of centrosymmetric zero-dimensional (0D) heterostructured core-shell PCP materials (Figure 1 a) led to the synergistic performance between the core framework (high storage capacity) and the shell framework (selectivity) within the heterogeneous material.<sup>[6,7]</sup> However, this centrosymmetric configuration always provides molecular transportation from the outer sphere to the center core but does not represent a permeable system through the material.<sup>[7]</sup> Heterogeneous porous materials with directional permeability are highly interesting for biological engineering and industrial applications such as separation, sensors, artificial cell membranes, or ion channels with tunable analyte affinity.<sup>[10]</sup>

Herein we show the fabrication of a two-dimensional (2D) binary Janus PCP system (Figure 1 b; binary Janus material consists of two separate systems, though in general Janus material can consist of two or more materials) by taking advantage of our knowledge about the immobilization of PCPs on a substrate by using liquid phase epitaxy (LPE).<sup>[11]</sup> We chose pillared-layer PCP systems:  $[\text{Cu}_2(\text{ndc})_2(\text{dabco})]_n$  (**A**) and  $[\text{Cu}_2(\text{NH}_2\text{-bdc})_2(\text{dabco})]_n$  (**B**) (ndc = 1,4-naphthalenedicarboxylate;  $\text{NH}_2\text{-bdc}$  = 2-amine-1,4-benzenedicarboxylate; dabco = 1,4-diazabicyclo[2.2.2]octane).<sup>[12]</sup> Both framework systems are tetragonal three-dimensional frameworks with paddlewheel dicopper units linked by dicarboxylates to form 2D square lattices, which are further interconnected by nitrogen pillar ligands. The framework **B** allows postsynthetic

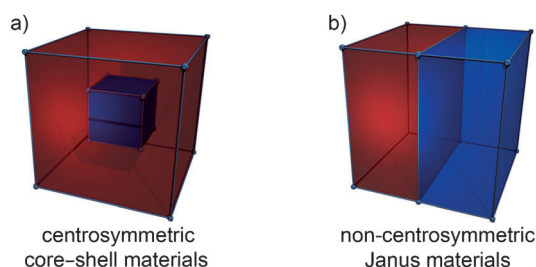


**Figure 1.** Schematic representation of centrosymmetric core-shell (a) and non-centrosymmetric Janus (b) heterostructured materials.

[\*] Dr. M. Meilikhov, Dr. S. Furukawa, Prof. S. Kitagawa  
Institute for Integrated Cell-Material Sciences (WPI-iCeMS)  
Kyoto University  
Yoshida, Sakyo-ku, Kyoto 606-8501 (Japan)  
E-mail: shuhei.furukawa@icems.kyoto-u.ac.jp  
Dr. S. Furukawa, Prof. S. Kitagawa  
ERATO Kitagawa Integrated Pores Project (Japan) Science and  
Technology Agency (JST), Kyoto Research Park Bldg #3  
Shimogyo-ku, Kyoto 600-8815 (Japan)  
K. Hirai, Prof. S. Kitagawa  
Department of Synthetic Chemistry and Biological Chemistry  
Graduate School of Engineering, Kyoto University  
Katsura, Nishikyo-ku, Kyoto 615-8510 (Japan)  
E-mail: kitagawa@sbchem.kyoto-u.ac.jp  
Prof. R. A. Fischer  
Department of Inorganic Chemistry II, Ruhr University Bochum  
Universitätsstrasse 150, 44780 Bochum (Germany)

[\*\*] M.M. is grateful to JSPS Postdoctoral Fellowship Program for foreign researchers. iCeMS is supported by World Premier International Research Initiative (WPI), MEXT (Japan). The authors thank Dr. Nobuhiro Morone and support from CeMI for assistance with measurement of FESEM.

Supporting information for this article is available on the WWW under <http://dx.doi.org/10.1002/anie.201207320>.

chemical modification (PSM) with succinic acid anhydride to form  $[\text{Cu}_2(\text{HOOC}(\text{CH}_2)_2\text{OCNH-bdc})(\text{NH}_2\text{-bdc})(\text{dabco})]_n$ , (C).<sup>[13]</sup> By using LPE and PSM we fabricated two Janus PCP materials with different deposition sequences on quartz crystal microbalance (QCM) sensors: Type I(C@A) and Type II(A@C), along with one type of homogeneous PCP material Type III(AC) (Figure 2). Mixture sorption experiments (that is, sorption experiments with compound mixtures) using QCM sensors for volatile organic compounds

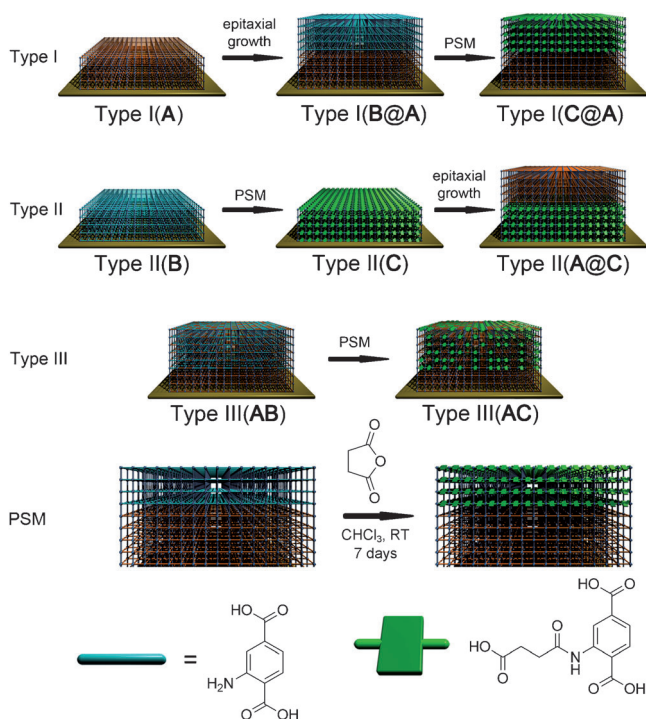


**Figure 2.** Different types of heterostructured Janus PCP coatings with PCP frameworks **A**:  $[\text{Cu}_2(\text{ndc})_2(\text{dabco})]_n$ ; **B**:  $[\text{Cu}_2(\text{NH}_2\text{-bdc})_2(\text{dabco})]_n$ ; **C**:  $[\text{Cu}_2(\text{HOOC}(\text{CH}_2)_2\text{OCNH-bdc})_2(\text{dabco})]_n$  and the principle of post-synthetic modification of Janus PCP coatings exemplarily demonstrated for Type I(B@A) material.

(VOCs) with different size and polarity have shown that the analyte affinity of sensor devices is tunable and depends on the sequence of heterogeneous Janus PCP coatings.

The key for framework design is the combination of one polar PCP (C) with a nonpolar PCP (A) within a heterogeneous Janus PCP material. Consequently, the final Janus PCP coatings can be regarded as amphiphilic materials. Janus PCP coating of Type I(C@A) or Type II(A@C) were built from the frameworks A and B, grown in an epitaxial way on top of each other, followed by the selective PSM to convert B to C. Note that both types exhibited the same chemical composition, but have two different spatial configurations, either face-up or face-down configuration. Type III(AC) PCP coatings consisted of statistically distributed apolar and polar ligands without spatial separation of distinct PCP systems.

All three different types of PCP coatings were deposited on the gold surfaces of QCM sensors that were modified by pyridyl-terminated self-assembled monolayers to achieve

oriented growth of the PCP coatings.<sup>[14]</sup> For the fabrication of Type I(C@A) by the LPE method, the framework A was immobilized in the first reaction step (25 cycles) followed by the epitaxial growth of the framework B (25 cycles) on top of A and finally the selective PSM to convert B to C (Figure 2). Type II(A@C) exhibits the inverse sequential order of the deposition (that is, A was epitaxially grown on top of C). For the fabrication of homogeneous PCP coatings of Type III(AC) with a statistical distribution of ndc and  $\text{NH}_2\text{-bdc}$  ligands throughout the entire system, the deposition was performed in one reaction step, in which the ligands were mixed in the solution, followed by the PSM. For the fabrication of all coatings (Type I, Type II, and Type III), a total number of 50 deposition cycles was performed, and thus the thickness of all final materials was about 50 nm. Note that for the fabrication of Type III coatings a seeding layer of A was necessary to achieve a crystalline and oriented PCP coating.

PCP coatings of all three types were characterized as described in previous reports.<sup>[15]</sup> The following text is a general description of material characterization applied for all three types of PCP coatings. The in situ monitoring of the immobilization process was achieved by liquid-phase QCM. The typical step curve of the time-dependent frequency change could be attributed to chemical deposition of material at the QCM sensor surface (Figure S3 in the Supporting Information). The crystallinity of binary Janus PCP coatings was confirmed by powder X-ray diffraction (PXRD) measurements. All obtained Janus PCP coatings were preferentially oriented into the [001] direction ( $2\theta = 9.12^\circ$ ) and with no clear preferential ordering in the lateral direction (Figure 3). The grazing incidence X-ray diffraction data supported this fact by exhibiting the 100 and 001 diffractions at the same time. The positions of the observed reflexes are consistent with the calculated PXRD pattern from the bulk  $[\text{Cu}_2(\text{ndc})_2(\text{dabco})]_n$  phase.<sup>[16]</sup> Field-emission scanning electron microscopy (FESEM) images provided evidence for the continuous coatings without any crack (Figure S2 in the Supporting Information). Infrared reflection absorbance spectroscopy (IRRAS) confirms the presence of the characteristic vibrational bands of the coordinated carboxylate groups in the region between 1500 and 1700  $\text{cm}^{-1}$  (Figure S1 in the Supporting Information). Additional vibrational bands at

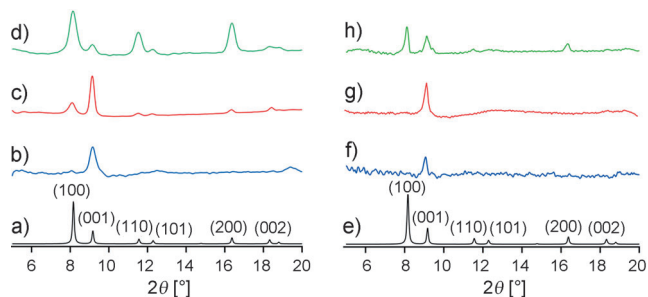


**Figure 3.** PXRD pattern of a) A (simulated one), b) Type I(A), c) Type I(B@A), and d) the grazing incidence PXRD pattern of Type I(C@A). PXRD pattern of e) A (simulated one), f) Type II(B) and Type II(C), g) Type II(A@C), and h) the grazing incidence PXRD pattern of Type II(A@C).

1453 and 1591  $\text{cm}^{-1}$  are attributed to the presence of the amine functional groups of the  $\text{NH}_2$ -bdc ligand, and the band at 1320  $\text{cm}^{-1}$  confirms the successful amide bond formation (the yield of PSM was reported as around 50%<sup>[13]</sup>).

The comparison of sorption properties between the non-centrosymmetric Type I/Type II materials and the homogeneous Type III material emphasizes the influence of different spatial configurations within the heterogeneous materials on the overall porous properties. Two VOCs with different size and polarity (methanol and hexane) were chosen for sorption experiments. Prior to sorption experiments, it was highly important to activate the PCP materials of all three types and remove all incorporated unreacted starting reagents and solvent molecules from the pores to be able to compare the sorption data of different materials. The activation process was examined in two steps. In the first step the coated QCM sensor was soaked in pure  $\text{CH}_2\text{Cl}_2$  for one hour at 40 °C and subsequently dried in an Ar stream. Additionally, the QCM sensors were placed inside the QCM chamber and heated at 70 °C in a He stream (100 sccm) for one additional hour. The adsorption isotherms were recorded at 25 °C using an environment-controlled QCM system<sup>[17]</sup> that controlled the partial vapor pressure of VOCs within the range of  $P/P_0 = 0$ –95 %.

Single-VOC sorption experiments (sorption experiments with one VOC) using Type I(**C@A**) and Type II(**A@C**) coatings revealed similar maximum methanol uptake of 1.2 molecules per copper dimer unit at  $P/P_0 = 95$  % (Figure 4). Both isotherms exhibited the type I sorption profiles typical

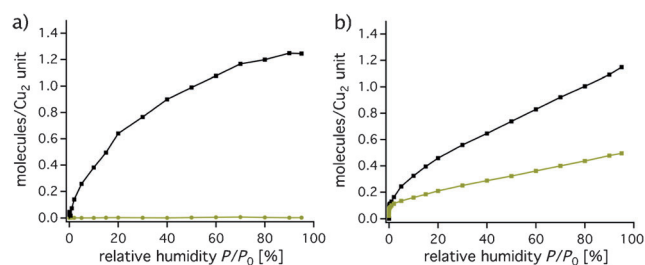


**Figure 4.** a) MeOH (black) and hexane (light brown) single-VOC adsorption isotherms of Type I(**C@A**) and b) MeOH (black) and hexane (light brown) adsorption isotherms of Type II(**A@C**).

for microporous materials. This fact indicated the preserved porosity of the heterostructured materials, though the PSM diminished the pore size by the introduction of additional carboxylic acid functionalities pointing into the pores. The adsorption characteristics for methanol as a small and polar VOC did not depend on the sequential arrangement of the frameworks **A** and **C**, since both PCP systems possessed the suitable pore size and polar environment for methanol accommodation. In contrast, the single-VOC sorption experiment of Type I(**C@A**) exhibited no uptake for hexane as a large and nonpolar VOC. When swapping the arrangement between **A** and **C**, a maximum amount of 0.5 hexane molecules per copper dimer unit could be adsorbed by Type II(**A@C**) material. This fact indicated that the narrow and polar pores of the upper part **C** of the binary Janus PCP

Type I(**C@A**) coatings with the framework **C** were inaccessible for hexane. The corresponding hexane adsorption measurement for single framework **C** exhibited no uptake for hexane, thereby further supporting this blocking effect. These results also suggest that the coating with 2D Janus PCP on the QCM sensor is perfectly achieved and there is no crack or lateral inhomogeneity that would allow for molecule permeation.

The results of single-analyte adsorption experiments indicated the possible selective adsorption properties of binary Janus PCP coatings. We performed multiple-VOCs sorption experiments to confirm and strengthen this assumption, since the performance of a porous material could strongly vary during single- and multiple-analyte sorption experiments. For mixture sorption experiments the relative concentration of one of the analytes was kept constant at the highest possible value ( $P/P_0 = 47.5$  % of relative concentration of the VOC), and the concentration of the second VOC was varied in the range between  $P/P_0 = 0$ –47.5 %. The limitation of the highest possible relative concentration at 47.5 % for a single VOC is caused by the fact that He is required as a carrier gas (minimum 5 % for a single analyte) and that the streams of methanol and hexane are combined before reaching the QCM cell (Figure S10 in the Supporting Information).

Interestingly, the sorption experiment of Type I(**C@A**), in which the relative concentration of hexane was kept constant at 47.5 % during the sorption for methanol, presented the typical type I sorption profile with a similar overall uptake of 0.32  $\text{g g}^{-1}$ , compared to the single-methanol sorption experiment for the same material ( $P/P_0 = 50$  %: overall uptake is 0.34  $\text{g g}^{-1}$ ; Figure 5 a). In contrast to this result, the adsorption isotherm obtained by keeping the methanol concentration at a constant value of 47.5 % and varying the hexane concentration from 0 to 47.5 % presented an initial huge uptake of 0.24  $\text{g g}^{-1}$  but did not change significantly during the increase of the hexane concentration to 47.5 % (Figure 5 b). The initial uptake was comparable to the uptake observed for methanol in the single-analyte sorption experiment, 0.34  $\text{g g}^{-1}$  at  $P/P_0 = 47.5$  % (Figure 4).

Mixture sorption experiments with Type II(**A@C**) provided a similar uptake profile to the one of Type I(**C@A**) for hexane with constant methanol concentration (Figure 5 b); the high initial uptake of molecules is caused by the constant concentration of MeOH or hexane, because the Type II-(**A@C**) could adsorb both analytes, and the overall uptake values did not change significantly during the increase of the concentration of the second VOC (Figure 5 c and d). Similar results were obtained for mixture sorption experiments with Type III(**AC**) materials (Figure S6 in the Supporting Information). Regarding all performed mixture sorption experiments, the isotherm with type I sorption profile was observed only for Type I(**C@A**) material, when the hexane concentration was kept constant and the methanol concentration was varied. This result clearly implies that the framework **C** located at the upper side of Type I(**C@A**) blocks the permeation for hexane into the material and selectively adsorbs the methanol molecules even in the mixture condition. For Type II(**A@C**) and Type III(**AC**) materials, owing



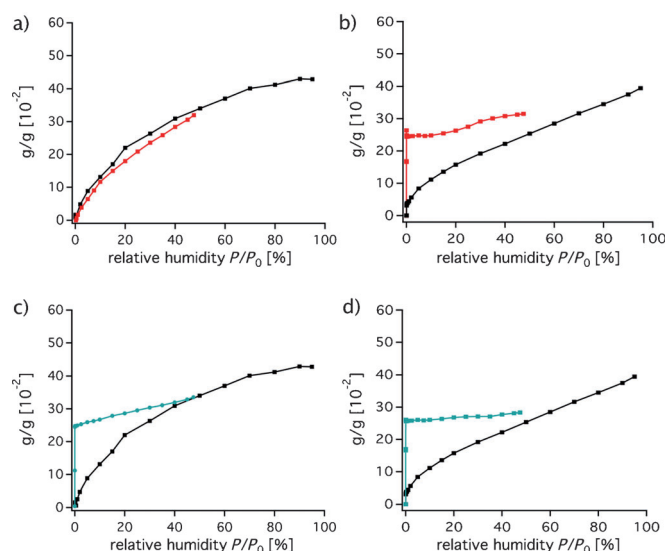


**Figure 5.** a) Comparison of MeOH single-VOC adsorption isotherm (black) and multiple-VOCs adsorption isotherm (red) with hexane vapor pressure  $P/P_0 = 47.5\%$  = constant and variable MeOH vapor pressure  $P/P_0 = 0-47.5\%$  for Type I(C@A). b) Comparison of MeOH single-VOC adsorption isotherm (black) and multiple-VOCs adsorption isotherm (red) with MeOH vapor pressure  $P/P_0 = 47.5\%$  = constant and variable hexane vapor pressure  $P/P_0 = 0-47.5\%$  for Type I(C@A). c) The comparison of the MeOH single-VOC adsorption isotherm of Type II(A@C) (black) and multiple-VOCs adsorption isotherm (blue) with hexane vapor pressure  $P/P_0 = 47.5\%$  = constant and variable MeOH vapor pressure  $P/P_0 = 0-47.5\%$  for Type II(A@C). d) The comparison of the MeOH single-VOC adsorption isotherm of Type II(A@C) (black) and multiple-VOCs adsorption isotherm (blue) with methanol vapor pressure  $P/P_0 = 47.5\%$  = constant and variable hexane vapor pressure  $P/P_0 = 0-47.5\%$  for Type II(A@C).

to the lack of the homogenous lateral coating of **A** with **C**, no blocking effect was observed, thus indicating the permeability of those materials for both analytes without any preference for one of them.

In conclusion, sophisticated heterostructured non-centrosymmetric binary Janus PCP coatings Type I(C@A) and Type II(A@C) with permanent porosity were fabricated. Both heterogeneous materials are based on structurally and topologically identical PCP systems of pillared-layer type  $[\text{Cu}_2(\text{dicarboxylate})_2(\text{dabco})]_n$  with variation of the dicarboxylate ligand. The precise investigations of adsorption properties of these heterostructured materials using QCM sensor devices exhibited tunable analyte affinity strongly depending on the upper surface functionality. The directional permeability and selective adsorption behavior were examined by changing the spatial arrangement of **A** and **C**. The Type I-(C@A) coatings could selectively adsorb the small and polar VOC methanol out of a mixture with hexane, however, the inversed structure of Type II(A@C) showed no selectivity. The comparison of heterogeneous, non-centrosymmetric Janus PCP coatings with homogeneous PCP coatings of Type III(AC) emphasized the impact of spatial separation of distinct PCP systems. This result clearly demonstrated that the heterogeneous hybridization concept (or the PCP-on-PCP concept) could be applied to device coatings for the precise tuning of sensing performance and will open the way

for the application of PCPs with higher chemical complexity in the field of electronics.<sup>[18]</sup>

Received: September 11, 2012

Published online: November 4, 2012

**Keywords:** coordination polymers · heterostructures · interfaces · metal–organic frameworks · surface modification

- [1] J. Du, R. K. O'Reilly, *Chem. Soc. Rev.* **2011**, *40*, 2402–2416.
- [2] T. Goldacker, V. Abetz, R. Stadler, I. Erukhivomic, L. Leibler, *Nature* **1999**, *398*, 137–139.
- [3] a) S. Alayoglu, A. U. Nilekar, M. Mavrikakis, B. Eichhorn, *Nat. Mater.* **2008**, *7*, 333–338; b) K. Maeda, K. Teramura, D. Lu, N. Saito, Y. Inoue, K. Domen, *Angew. Chem.* **2006**, *118*, 7970–7973; *Angew. Chem. Int. Ed.* **2006**, *45*, 7806–7809; c) A. Harada, K. Kataoka, *Science* **1999**, *283*, 65–67.
- [4] a) J. Zhang, X. J. Wang, D. X. Wu, L. Hiu, H. Y. Zhao, *Chem. Mater.* **2009**, *21*, 4012–4018; b) F. Schacher, E. Betthausen, A. Walther, H. Schmalz, D. V. Pergushov, A. H. E. Mueller, *ACS Nano* **2009**, *3*, 2095–2102.
- [5] a) S. Jiang, Q. Chen, M. Tripathy, E. Luijten, K. S. Schweizer, S. Granick, *Adv. Mater.* **2010**, *22*, 1060–1071; b) A. Walther, A. H. E. Müller, *Soft Matter* **2008**, *4*, 663–668.
- [6] K. Hirai, S. Furukawa, M. Kondo, M. Meilikhov, Y. Sakata, O. Sakata, S. Kitagawa, *Chem. Commun.* **2012**, *48*, 6472–6474.
- [7] K. Hirai, S. Furukawa, M. Kondo, H. Uehara, O. Sakata, S. Kitagawa, *Angew. Chem.* **2011**, *123*, 8207–8211; *Angew. Chem. Int. Ed.* **2011**, *50*, 8057–8061.
- [8] a) O. M. Yaghi, M. O'Keeffe, N. W. Ockwig, H. K. Chae, M. Eddaoudi, J. Kim, *Nature* **2003**, *423*, 705–714; b) S. Kitagawa, R. Kitaura, S. Noro, *Angew. Chem.* **2004**, *116*, 2388–2430; *Angew. Chem. Int. Ed.* **2004**, *43*, 2334–2337; c) G. Férey, C. Mellot-Draznieks, C. Serre, F. Millange, *Acc. Chem. Res.* **2005**, *38*, 217–225; d) Z. Wang, S. M. Cohen, *Chem. Soc. Rev.* **2009**, *38*, 1315–1329; e) M. Dincă, J. R. Long, *Angew. Chem.* **2008**, *120*, 6870–6884; *Angew. Chem. Int. Ed.* **2008**, *47*, 6766–6779; f) R. E. Morris, P. S. Wheatley, *Angew. Chem.* **2008**, *120*, 5044–5059; *Angew. Chem. Int. Ed.* **2008**, *47*, 4966–4981; g) D. Zacher, O. Shekhah, C. Wöll, R. A. Fischer, *Chem. Soc. Rev.* **2009**, *38*, 1418–1429.
- [9] a) S. Furukawa, K. Hirai, K. Nakagawa, Y. Takashima, R. Matsuda, T. Tsuruoka, M. Kondo, D. Tanaka, H. Sakamoto, S. Shimomura, O. Sakata, S. Kitagawa, *Angew. Chem.* **2009**, *121*, 1798–1802; *Angew. Chem. Int. Ed.* **2009**, *48*, 1766–1770; b) S. Furukawa, K. Hirai, Y. Takashima, K. Nakagawa, M. Kondo, T. Tsuruoka, O. Sakata, S. Kitagawa, *Chem. Commun.* **2009**, 5097–5099.
- [10] a) I. K. Voets, R. Fokkink, T. Hellweg, S. M. King, P. de Waard, A. de Keizer, M. A. C. Stuart, *Soft Matter* **2009**, *5*, 999–1005; b) J. Choi, Y. Zhao, S. Chien, Y.-H. Lo, *Nano Lett.* **2003**, *3*, 995–1000.
- [11] a) D. Zacher, K. Yusenko, A. Betard, S. Henke, M. Molon, T. Ladnorg, A. Shekhah, B. Schüpbach, T. de Los Arcos, M. Krasnopolski, M. Meilikhov, J. Winter, A. Terfort, C. Wöll, R. A. Fischer, *Chem. Eur. J.* **2011**, *17*, 1448–1455; b) O. Shekhah, K. Hirai, H. Wang, H. Uehara, M. Kondo, S. Diring, D. Zacher, R. A. Fischer, O. Sakata, S. Kitagawa, S. Furukawa, C. Wöll, *Dalton Trans.* **2011**, *40*, 4954–4958.
- [12] K. Seki, W. Mori, *J. Phys. Chem. B* **2002**, *106*, 1380–1385.
- [13] S. J. Garibay, Z. Wang, K. K. Tanabe, S. Cohen, *Inorg. Chem.* **2009**, *48*, 7341–7349.
- [14] E. Biemmi, C. Scherb, T. Bein, *J. Am. Chem. Soc.* **2007**, *129*, 8054–8055.

- [15] a) O. Shekhah, H. Wang, S. Kowarik, F. Schreiber, M. Paulus, M. Tolan, C. Sternemann, F. Evers, D. Zacher, R. A. Fischer, C. Wöll, *J. Am. Chem. Soc.* **2007**, *129*, 15118–15119; b) K. Yussenko, M. Meilikhov, D. Zacher, F. Wieland, C. Sternemann, X. Stammer, T. Lahnorg, C. Wöll, R. A. Fischer, *CrystEngComm* **2010**, *12*, 2086–2090; c) O. Shekhah, H. K. Arslan, K. Chen, M. Schmittl, R. Maul, W. Wenzel, C. Wöll, *Chem. Commun.* **2011**, 47, 11210–11212.
- [16] K. Seki, *Langmuir* **2002**, *18*, 2441–2443.
- [17] H. Uehara, S. Diring, S. Furukawa, Z. Kalay, M. Tsotsalas, M. Nakahama, K. Hirai, M. Kondo, O. Sakata, S. Kitagawa, *J. Am. Chem. Soc.* **2011**, *133*, 11932–11935.
- [18] P. Falcaro, D. Buso, A. J. Hill, C. M. Doherty, *Adv. Mater.* **2012**, *24*, 3153–3168.
-